Ultrasonically spray coated silver layers from designed precursor inks for flexible electronics

Peer-reviewed author version

MARCHAL, Wouter; VANDEVENNE, Glen; D'HAEN, Jan; Calmont de Andrade Almeida, A.; Durand Sola Jr, M.A.; VAN DEN HAM, Jonathan; DRIJKONINGEN, Jeroen; ELEN, Ken; DEFERME, Wim; VAN BAEL, Marlies & HARDY, An (2017)
Ultrasonically spray coated silver layers from designed precursor inks for flexible electronics. In: NANOTECHNOLOGY, 28(21), p. 1-12 (Art N° 215202).

DOI: 10.1088/1361-6528/aa6d3a
Handle: http://hdl.handle.net/1942/23735

Ultrasonically spray coated silver layers from designed precursor inks for flexible electronics

W. Marchal[1,4], G. Vandevenne[2,4], J. D'Haen[3,4], A. Calmont de Andrade Almeida[1], M. A. Durand Sola jr.[2], E.J. van den Ham[1,4], J. Drijkoningen[2,4], K. Elen[1,4], W. Deferme[2,5], M.K. Van Bael[1,4], A. Hardy[1,4]

[1] UHasselt, Hasselt University, Institute for Materials Research(IMO-IMOMEC), Inorganic and Physical chemistry, Agoralaan, 3590 Diepenbeek, Belgium
[2] UHasselt, Hasselt University, Institute for Materials Research (IMO-IMOMEC), Engineering Materials and Applications, Agoralaan, 3590 Diepenbeek, Belgium
[3] UHasselt, Hasselt University, Institute for Materials Research (IMO-IMOMEC), Materials Physics, Agoralaan, 3590 Diepenbeek, Belgium
[4] IMEC vzw, division IMOMEC, Agoralaan, 3590 Diepenbeek, Belgium
[5] Flanders make vzw, Oude Diestersebaan 133, 3920 Lommel, Belgium
[*] Corresponding author: An.Hardy@uhasselt.be; Tel.: +32(0)11268308

Abstract

Integration of electronic circuit components onto flexible materials such as plastic foils, paper and textiles is a key challenge for the development of future smart applications. Therefore, conductive metal features need to be deposited on temperature sensitive substrates in a fast and straightforward way. The feasibility of these emerging (nano-) electronic technologies depends on the availability of well-designed deposition techniques and on novel functional metal inks. As ultrasonic spray coating (USSC) is one of the most promising techniques to meet the above requirements, innovative metal organic decomposition (MOD) inks are designed to deposit silver features on plastic foils. Various amine ligands were screened and their influence on the ink stability and the characteristics of the resulting metal deposition was evaluated to determine the optimal formulation. Eventually, silver layers with excellent performance in terms of conductivity (15 % bulk silver conductivity), stability, morphology and adhesion could be obtained, while operating in a very low temperature window of 70-120 °C. Moreover, the optimal deposition conditions were determined via an in-depth analysis of the ultrasonically sprayed silver layers. Applying these tailored MOD inks, the ultrasonic spray coating (USSC) technique enables smooth, semi-transparent silver layers with a tunable thickness on large areas without time-consuming additional sintering steps after deposition. Therefore, this novel combination of nanoparticle-free Ag-inks and the USSC process holds promise for high throughput deposition of highly conductive silver features on heat sensitive substrates and even 3D objects.

Introduction

In view of the recent innovation trend towards the 'internet of things' (IOT), the facile integration of electronic circuits onto cheap, light-weight and flexible materials (plastics, textiles, paper,…) will be of great importance. In this framework, research on the scalable, straightforward and low-temperature deposition of metallic nanostructures such as thin silver layers is key. Having the highest electric conductivity of all metals and an intrinsic resistance against oxidation, silver can play a considerable role in future applications including wearables [1], sensors [2] (smart skins, packaging,

textiles…), flexible photovoltaics [3], RFID tags [4], and other applications. Moreover, as role to role (R2R) manufacturing is targeted for high volume deposition and cost effectiveness, suitable printing techniques are being explored intensively.[5-9] Printing allows to deposit the material only, and exactly, where it is required for the application, without ink dissipation as in spin coating followed by lithography. This, of course, necessitates the availability and development of performant silver inks.

The majority of the reported printable silver inks consist of micro- and nanoparticles, which are dispersed in an optimized solvent blend to acquire a smooth and uniform deposition [10] by balancing the evaporation-induced radial flow (resulting in the coffee-stain effect) and Marangoni flow recirculation. [6] Moreover, parameters such as Ohnesorge/Fromm number (preventing satellite formation [11,12]) and the wetting on the investigated substrate need to be taken into account when optimizing an ink for inkjet printing. Besides the aforementioned components, particle-based inks contain organic- or polymer-based stabilizers [13], dispersing agents and surfactants. After ink deposition, these constituents need to be removed because of their unfavorable influence on the resulting conductivity of the layer. Moreover, the layers require sintering to enhance the formation of conductive pathways between the particles. In order to obtain electrically conductive silver features, a wide variety of curing techniques can be applied. The most straightforward method is thermal sintering. However, elevated temperatures (150 – 400 °C) which are not compatible with flexible substrates (such as Polyethylene Terephthalate: PET) are necessary to attain a satisfying conductivity.[14-18] This is mainly due to the high decomposition temperature of the stabilizing agents while the actual sintering of silver (nano-) particles would occur at relatively low temperature (Gibbs-Thompson effect).[19-21] Laser and infrared sintering techniques are designed to specifically heat the deposited layer without deteriorating the underlying substrate.[22-24] The main drawback of lasers for large area applications is the limited spot size.[7] In addition, combined curing methods can be applied (e.g. combining thermal and UV curing)[25] or more capital-intensive or complex methods were demonstrated such as flash sintering [26,27]. Alternatively, self-sintering mechanisms based on the desorption of stabilizers [28] or charge neutralization on the particle surface are clever tricks to overcome the need for a high-temperature sintering step.[20,29] In this way, conductive silver features can be obtained from particle-based inks at temperatures well below 150 °C, or even at room temperature [28].

In addition, an alternative class of inks was introduced, based on solutions of metal complexes, which keeps on receiving more scientific attention in the last years. These innovative particle-free inks are often referred to as Metal Organic Decomposition (MOD) inks.[30,31] The solutions contain metal ions (mostly Ag^+), which are coordinated with electron donating ligands. Frequently used coordination agents are amine containing ligands, although silver complexes with sulfur and oxygen containing electron donating groups are also reported.[32,33] Moreover, a reducing agent is present, which will convert the Ag^+ ions to metallic silver during or after the printing process at room temperature to slightly elevated temperatures (< 150 °C). Thus, the thermal sintering temperature window to obtain silver layers with a comparable resistivity to evaporated silver depositions is generally lower for MOD inks compared to silver dispersion inks. Walker and Lewis [34] synthesized an ink based on a modified Tollens process. This ink enabled reaching bulk silver conductivity (6.25 10^5 S/cm) values after inkjet printing and curing at 90 °C for 15 minutes. Multiple other articles also report on the possibility to obtain highly conductive silver layers (10 % - 100 % of bulk silver conductivity) on flexible substrates at very low temperatures (RT-150 °C), combining different silver reagents and coordinating/reducing agents.[35-42] Besides the possibility to apply simple thermal or

infrared sintering on common plastic substrates, which is interesting for industrial production because of limited investment costs, MOD inks offer additional benefits: clogging in the printer nozzle can be prevented as no particle coagulation can occur.

As large area applications and R2R high-throughput processing will gain importance, transferring lab-scale printing protocols to industrial environments is necessary. Ultrasonic spray coating (USSC) is a very versatile deposition technique, able to process entire devices comprising of various materials such as OPVs [43-45] and OLEDS.[46] Although each printing technique has its own advantages, disadvantages and consequently its specific applications, the USSC method was selected in this study as it allows a very high deposition speed [47] and the layer thickness can be easily adjusted by changing the number of passes, the flow rate or the ink concentration. Moreover, patterning and coating on virtually any substrate is possible [48], including 3D structures.[49] Finally, USSC has the additional benefit of being capable to effectively deposit inks with multifarious rheological properties [50]. Due to these inherent benefits of the USSC technique, the deposition of silver nanoparticle inks was already reported in various studies. Girotto *et al. [51]* obtained resistivity values of 40-100 μΩ cm (25 – 60 times bulk silver conductivity) after annealing the deposited silver prints at 150 °C for only few seconds. At lower temperatures, higher annealing times were required or a higher resistivity was observed. Ankireddy *et al. [52]* obtained superior resistivity values (10-87 % of silver bulk conductivity), at the cost of higher sintering temperatures (130 – 250 °C) and times (up to 210 minutes). To improve the silver layer properties and process parameter trade-off, a low-temperature (< 120 °C) USSC deposition of an optimized, particle-free MOD ink is reported for the first time. During the deposition process, the MOD precursor is ultrasonically nebulized, atomized and directly guided via a nitrogen gas shroud onto a pre-heated substrate.

As USSC is a completely different deposition technique compared to inkjet printing, the ink compositions concentrations and solvents were carefully redesigned. Simply transferring inkjet ink synthesis protocols from literature results in very rough, thick and opaque coatings according to our experiments. To resolve this issue, the ink properties need to be changed, including the Ag complexes and the ink's load. First, a screening of various amine based ligands was performed which coordinate the silver acetate starting salt (amino-alcohols [53], heterocyclic amines [54],[55],…). In addition, the loading of the silver spray coat inks was adjusted compared to conventional inkjet MOD inks and simple low-boiling alcohol-based solvent systems were used. In this way, transparent, low-viscous silver solutions which can be easily atomized ultrasonically in the spray coater setup, were obtained. In all cases, a large excess of ligand was added to prevent Ag_2O precipitation and to assure that all silver ions are coordinated. Hence, the ligands are able to protect the Ag^+ ions from direct reduction in solution (before printing) in the presence of formic acid which is used as a reducing agent. On the other hand, slightly elevated temperatures suffice to start the reduction process, and can be used to initiate conversion to metallic Ag when desired.

A series of various amine ligands was investigated in the process of designing a high-performing MOD ink for USSC deposition. Differences in ligand polarity and ligands with additional hydroxide groups, making them possibly polydentate, were investigated. In addition, the effect of a varying number of substituents on the amine group (primary, binary, ternary amines) influencing the Lewis base strength was explored. The higher basicity of ternary amines and it's enhanced electron-donating coordination may influence the ink stability and decomposition temperature. The used ligands include ammonia (NH_3), hexylamine (hex), 2-amino-2-methyl-1-propanol (AMP), ethanolamine (EA),

morpholine (morph) and pyridine (pyr). Based on the studied properties (stability, decomposition) of all these silver complex containing inks and their resulting silver layers, convergence to an applicable, high-performance USSC ink was reached. Eventually, thin silver layers (110 nm) with a resistivity of $10.9 \cdot 10^{-8}$ Ω·m (approx. 15% bulk conductivity) could be obtained at temperatures as low as 120 °C without time-consuming post-annealing or curing steps. This set of high-performing properties, combined with a straightforward ink synthesis, fast and scalable deposition and 3D compatibility demonstrates the applicability of the novel MOD ink and USSC combination for various research domains.

Experimental

MOD ink synthesis

0.085 g of silver acetate (98 %, for synthesis, Merck, abbreviation: Ag(ac)) was dispersed in 20 ml ethanol (absolute, VWR) under stirring. The amine ligands were added dropwise in a 1:5 molar ratio (or 1:10 ratio) to the silver acetate and stirred until complete dissolution occurs, and a clear colorless solution is obtained. The employed amine ligands include hexylamine (99 %, Acros Organics), ethanolamine (>99.5 %, Sigma-Aldrich), 2-amino-2-methyl-1-propanol (> 99.0 %, Fluka), ammonia (25 % solution in water, pro analysis, Merck), morpholine (>99 %, for synthesis, Merck) and pyridine (99 %, extra pure, Acros Organics). Subsequently, formic acid (98 %, pro analysis, Sigma-Aldrich) was added to the mixture in a 1:1 molar ratio with silver acetate. This addition yields a miniscule amount of precipitation, which re-dissolves upon continuous stirring. The solution was transferred into a 50 ml volumetric flask and ethanol was added to obtain a 0.01 M silver solution.

Ultrasonic Spray Coating

The MOD inks described above were loaded in a syringe and deposited using an ultrasonic spray coater (Exacta Coat, Sono-Tek cooperation) with an accumist nozzle (Sono-Tek cooperation). The nitrogen carrier gas pressure to create an MOD ink aerosol was set to 1.5 psi, and the atomization power was 2 W. The spray nozzle was positioned at a distance of 6.9 cm from the hotplate surface, which was set at a deposition temperature between 70 °C and 120 °C, and moved with 50 mm s^{-1}. The ink was dispensed at 0.25 ml min^{-1} and the nozzle trajectory was repeated 20 times with a waiting time of 5 s between two passes. The above mentioned parameters apply for all investigated layers unless explicitly mentioned otherwise . The PET substrate (Melinex 125) surfaces were treated with a corona discharge (Electro-Technic Products, Model BD-20) before coating. No post treatment of the silver layers was required after the USSC process was completed.

Characterization

Fourier Transform Infrared (FTIR) analysis was carried out using a Bruker Vertex 70 spectrometer. For analysis of the silver precipitation, the degraded MOD precursors were filtrated whereupon the filtrate was washed with n-hexane. The precipitate was subsequently diluted with KBr (FTIR grade, >99 %, Sigma-Aldrich), grinded and pressed into a pellet (3 tons, 1-minute waiting time). For the temperature dependent FTIR study of the $Ag(hex)_x$ and $Ag(AMP)_x$ decomposition, the 5 ml corresponding MOD ink was transferred to a petri dish and put on a hotplate at the indicated temperature for 1 hour. Likewise, the precipitate was incorporated in a KBr pellet. Measurements were performed using a scan range of 4000-400 cm^{-1} with a spectral resolution of 4 cm^{-1} (32 scans).

Cyclic voltammetry was performed in a standard 3-electrode set-up with an Autolab PGstat128N potentiostat. 0.01 M solutions of the active silver species were prepared in 0.1 M KNO_3 solutions (10 % water/90 % ethanol) as supporting electrolyte. Measurements were conducted using a Pt wire working and Pt grid counter electrode, together with an Ag/AgCl reference electrode with e scan speed of 50 mV/s. Contact angle measurements were conducted with highly concentrated silver complex solutions (approx. 1.5 M) on a dataphysics system with OCA20 software is sessile drop modus. The droplet volume was set to 1 µl and the dispensing speed on 'slow'. X-ray Diffraction was performed with a Bruker D8 Discover apparatus using Cu-K_α radiation.

The decomposition of the silver inks was probed via TGA-DSC measurements (Q600, SDT, TA instruments, dry air 100 ml min^{-1}, heating rate: 5 °C min^{-1}) on dried MOD ink (RT – 60 °C). After deposition, the silver layers were prepared according to the ISO 2409 procedure for adhesion evaluation.[56] Cross cut patterning (spacing 2 mm) of the silver deposition on the PET substrate was followed by applying a standardized tape and inspection of the surface upon its removal. The obtained silver layers were characterized by atomic force microscopy (AFM) (Bruker, multi-mode 8 microscope, JVLR piezo large area scanner: 10 – 150 µm) in both tapping mode (Bruker Sb doped Si Tap525A tip, spring constant 200 N/m) and peakforce qualitative nanoscale mechanical mode (PF-QNM,). A non-calibrated Bruker silicon tip (k = 0.4 N/m) on a nitride lever was used (qualitative results between different areas are only compared within the same image). The sheet resistance was recorded by a homebuilt four-point probe Vanderpauw setup (Keithley 2400 source-, 2000 multi- and 7001 switch meter). Optical microscope images were collected with an Axiovert 40 MAT (Zeiss).

The morphology of the layers was further explored by means of scanning electron microscopy (SEM, FEI Quanta 200F FEG-SEM), equipped with an Energy Dispersive X-ray spectroscopy (EDX, EDAX TEAM EDS equipped with Octane Plus detector) detector to verify the local elemental composition. SEM and EDX measurements were carried out with an acceleration voltage of 10 kV unless mentioned otherwise. The thickness of the layers could be verified by imaging the cross section prepared via microtome cutting (Leica ultra cryomicrotome), whereupon the samples were visualized by cross sectional-transmission electron microscopy (X-TEM, FEI Tecnai Spirit, 120 kV acceleration voltage).

Results and discussion

MOD ink properties

Needless to say, the stability of the MOD precursors is of utmost importance for its possible future application as commercial silver ink. A fortiori during the USSC process, as clogging of the nozzle due to a limited ink stability would be a major bottleneck. In this respect, the stability of the freshly prepared silver MOD inks with the aforementioned ligands was evaluated in various storage conditions. The silver inks (with [Ag:ligand] = [1:10] ratio) were stored in ambient (daylight at 25 °C), dark (at 25 °C) and refrigerator (dark, 5 °C) conditions as silver acetate is reported to be highly photosensitive.[57-59] Stability values were measured in days starting from the complete synthesis of the silver ink until the occurrence of optically visible precipitation. Figure 1 indicates that both $Ag(morph)_x$ and $Ag(pyr)_x$ inks are very unstable and degrade almost immediately after formulation in all storage conditions. It is also remarkable that the most unstable inks contain ligands which don't have a primary amine functionality (morpholine and pyridine). Therefore, the silver morpholine and

silver pyridine inks could be eliminated from further in-depth investigation as their stability is too low for possible applications. All other silver inks remain stable for a longer period, especially if stored at 5 °C. Hence, the use primary amines for Ag MOD ink synthesis can be recommended. The presence of light however, has a less pronounced effect. For now, we can conclude that mainly the storage temperature is an important parameter to increase the ink shelf life. Moreover, the inks remain stable for several months without the addition of formic acid, which can be added just before the printing process to prolong the shelf life. The shelf life in an cooled environment is comparable with reported stabilities for nanoparticle inks.[42,52]

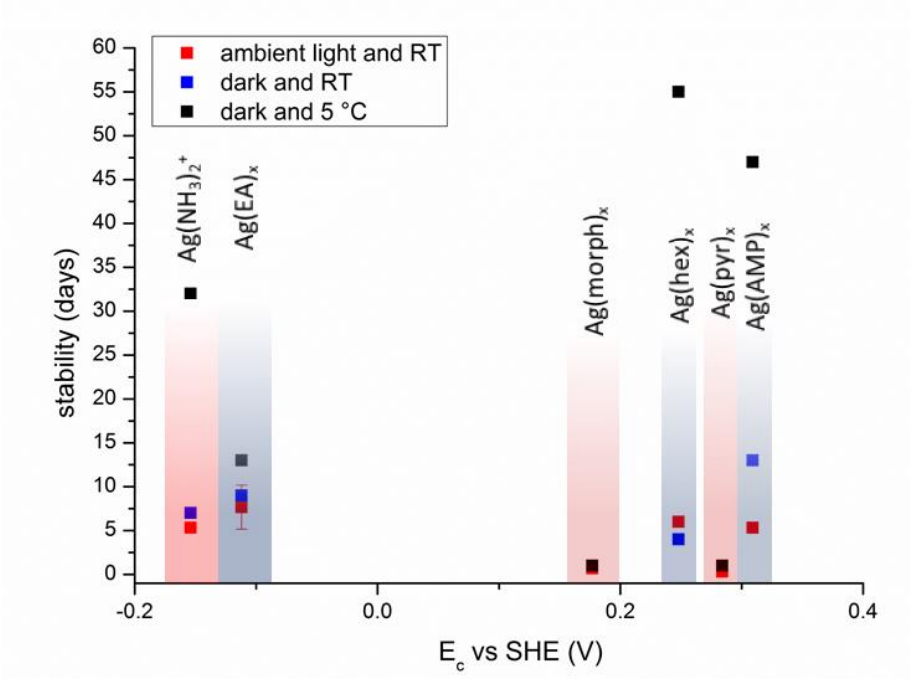

Figure 1: The ink lifetime is clearly higher in dark and 5 °C storage conditions for al inks containing ligands with primary amines. Moreover, there is no clear correlation between the stability and the cathodic reduction potential (E_c) versus the standard hydrogen electrode (SHE).

Moreover, the nature of this precipitation was investigated for all inks by means of infrared spectroscopy (Figure S1). All spectra show the absence of vibrationally active species besides of the background signals. Indeed, no signs of Ag_2O (signal at 535 cm^{-1}) or Ag_2CO_3 (peaks at 1410 cm^{-1}, 1020 cm^{-1}, 880 cm^{-1} and 690 cm^{-1}) could be observed.[60] Furthermore, the absence of peaks corresponding to the used amine ligands is demonstrated. Therefore, the solubility of the formed silver complex (depending on the ligand used) in the employed solvent (ethanol) is not the limiting factor for the precursor stability. As it can be concluded that the precipitate is metallic silver, additionally demonstrated by XRD (Figure S2), the reduction of the silver ion complex to the metallic species was identified as the stability-limiting phenomenon. To assess this stability against reduction in a more quantitative way, cyclic voltammetry experiments (Figure S3) were conducted on all silver inks to assess the reduction potential of the silver-amine [$Ag(lig)_x$] complexes. Figure 1 includes the varying cathodic reduction potentials, suggesting that the silver ions are in fact surrounded by the different ligands. The observed decrease of the cathodic reduction potential for all Ag^+ complexes compared to uncoordinated silver acetate (Figure S4) illustrates the coordination with the electron donating amine ligands. However, no obvious correlation between the cathodic reduction potential and the stability can be extracted. Otherwise it would be expected that the $Ag(NH_3)_2^+$ complex should

have the longest lifetime because its relatively low potential to reduce. This observation suggests that the activation energy of the reduction process plays an important role in the lifetime. Another indication for this kinetic effect is the huge difference in stability values for RT and 5 °C storage conditions.

Layer adhesion

The quality and applicability of the different stable silver MOD inks (containing NH_3, AMP, EA and hexylamine ligands) were estimated by testing the adhesion of the resulting silver layers on PET (Figure 2 right). Figure 2 (left) shows a microscope image of an ultrasonically spray coated silver hexylamine ink layer deposited at 100 °C after the adhesion test. In general, all the layers fit the classification of 1 on the appearance-based adhesion scale (from 0 to 5), which means all the layers exhibit a very limited detachment from the surface (all pictures are shown in supporting information Figure S5). However, to evaluate the adhesion between subsequently deposited silver layers (intra-layer adhesion), careful inspection of the tape after removal from the surface is required to guarantee that no silver is removed. In other words, both the cross cut image and the tape need to be checked before layer peel off can be ruled out. Upon tape examination, no residuals of the silver layers could be observed, except for the $Ag(NH_3)_2$ based MOD ink. A picture of the tape is included in figure 2 (left inset) to illustrate the unfavorable intra-layer adhesion.

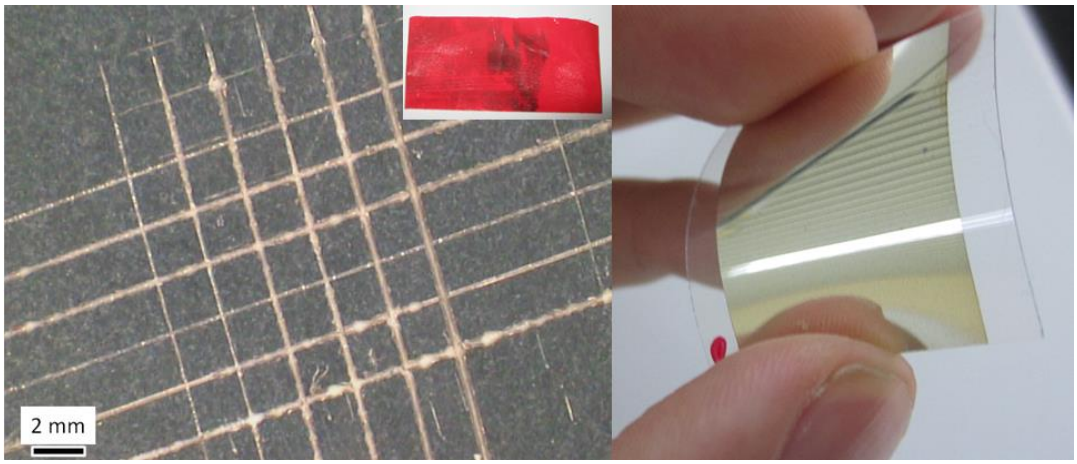

Figure 2: Cross cut pattern showing an adhesion of 1 according to the ISO 2409 classification (left), Inspection of the tape shows a poor intra layer adhesion for the $Ag(NH_3)_2^+$ based inks (inset left). The silver layers generally are very reflective and uniform (right) however differences exist depending on the used silver complex inside the 100 % ethanol based MOD ink.

The silver layers obtained from the various MOD inks slightly differ in appearance, more specifically in reflectance and uniformity. Since smooth and homogeneous silver depositions are targeted, a quantitative approach to determine the layer morphology was performed. Figure 3 presents the RMS roughness values of silver layers deposited at 100 °C from a 100% ethanol solution for different silver complexes. Results indicate that the $Ag(hex)_x$ and $Ag(AMP)_x$ based inks hold the most promise to achieve smooth silver depositions. This observation is remarkable as these ligands have the highest carbon content of the screened ligands. The smoother depositions suggest an enhanced interaction of the alkyl groups of the ligand with the PET substrate. This hypothesis is supported by contact angle measurements of the various silver complex ink on PET substrates (Figure S6). A highly concentrated solution of the complexes was used to verify the interactions with the substrate as the alcohol

solvent is expected to be largely evaporated in the atomization process during USSC. The $Ag(hex)_x$ ink exhibits the lowest contact angle on the PET substrates, followed by $Ag(AMP)_x$.

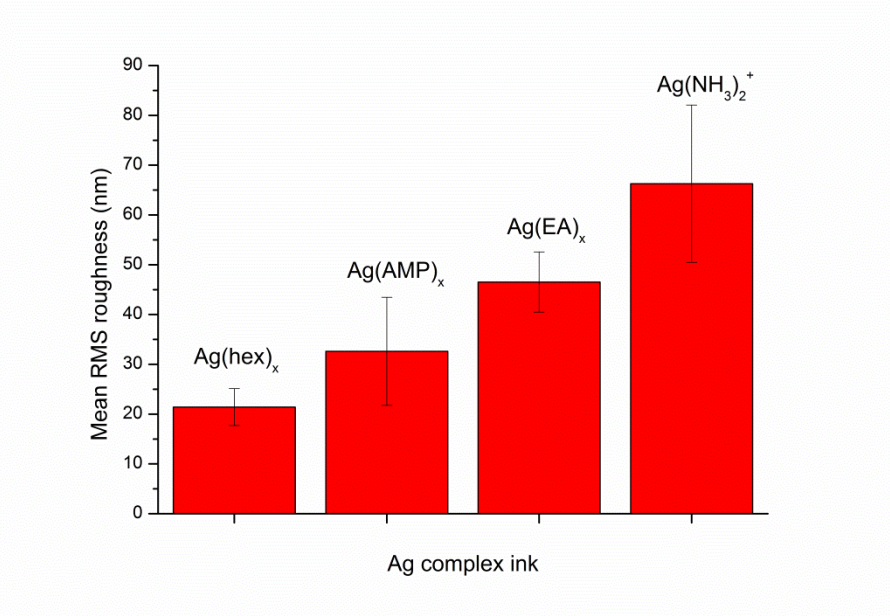

Figure 3: Mean RMS roughness of silver layers deposited at 100 °C. These values recorded via AFM measurements (at least 4 images per sample) show a trend towards increased smoothness for silver complexes containing amine ligands with a larger carbon chain.

To demonstrate the necessity of redesigning the MOD inks for USSC, the $Ag(NH_3)_2$-based MOD ink described by Walker and Lewis[34] was reproduced and spray coated (power 2.6 W, 0.25 ml min^{-1}, 5 passes). Although the ink performs very well in an inkjet setup according to their experiments and can be spray coated without practical issues, the deposited layers exhibit unfavorable properties. On corona-cleaned PET surfaces subjected to 120 °C, silver layers with a RMS roughness of 7765 nm ± 1084 nm were obtained. This high value is most probably caused by unfavorable wetting, high concentration and sub-optimal nebulization process. Pictures and profilometry data are presented in Figure S7, and comparison with the picture in Figure 2 clearly illustrates the tremendous improve that has been made by changing the ligands, solvent and concentration of the MOD ink, to be compatible with the USSC process.

The $Ag(hex)_x$ and $Ag(AMP)_x$ containing inks were selected for a more elaborate study and optimization as they exhibit an acceptable stability, very good adhesion to PET substrates and the lowest roughness values of all the tested samples. Optimization of the deposition temperature, in-depth morphological characterization and analysis of the resistivity was performed.

The temperature window in which the PET substrates were heated during silver deposition was confined between 70 and 120 °C. The lower temperature limit of 70 °C is necessary to activate the decomposition of the MOD ink, removing the organic content. The top limit of 120 °C was set to prevent thermal deformation of the substrate. Figure 4 shows the sheet resistance of the deposited silver layers from $Ag(hex)_x$ and $Ag(AMP)_x$ respectively. A general decreasing trend in sheet resistance towards higher deposition temperatures can be observed for both inks. The reducing sheet resistance trend is more evident for the AMP based ink compared to the hexylamine ink. This can be explained by the higher boiling point of AMP compared to hexylamine, which are both present in

excess. Indeed, TGA-DSC results clearly indicate that the $Ag(hex)_x$ inks reach their residual mass (pure silver) before $Ag(AMP)_x$ inks do (Figure S8). Hence, the principal mass loss for both MOD inks is associated with an endothermal phenomenon, pointing to ligand evaporation besides the acetate and formate decomposition. At 80 °C, a significant fraction of the AMP ligand will remain present in the silver layer after USSC which diminishes the conductivity, whereas the majority of the hexylamine is already evaporated in comparable experimental conditions. The fact that no weight loss is observed after 150 °C for both inks is supplementary evidence for the interaction between the silver complexes and the formate as pure silver acetate decomposes at higher temperatures.[61,62]

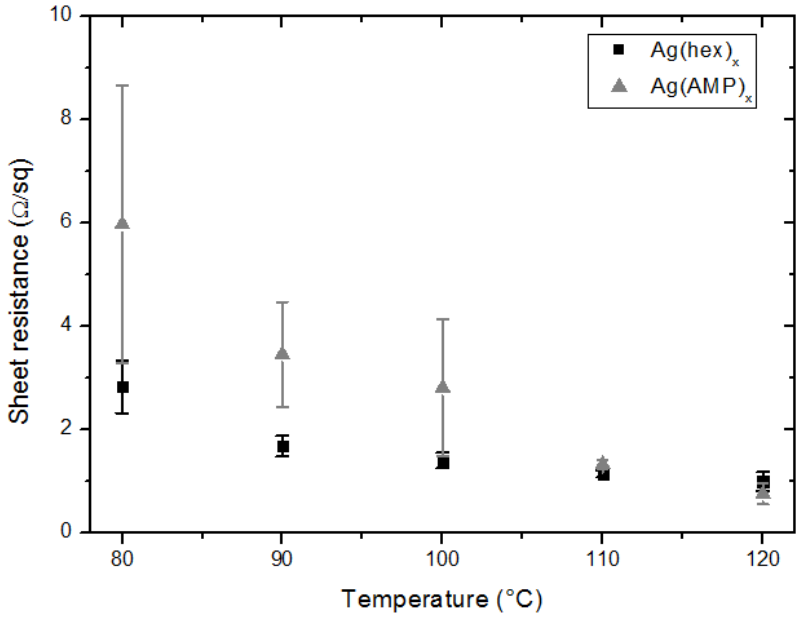

Figure 4: Higher deposition temperatures decrease the sheet resistance of the resulting silver layers because of a more efficient removal of the organic amine ligands. The error bars depict the standard deviations on the plotted average values for at least 4 individual measurements on different substrates. Spray coat parameters: flow rate = 0.25 ml/min, path speed 50 mm/s, 20 passes, 5 s waiting time between passes.

To fortify the claim that the decrease of the sheet resistance is mainly due to the removal of organic components inside the MOD ink, infrared spectra (FTIR) were recorded at several temperatures inside the employed experimental window (80 °C – 120 °C, Figure 5). Moreover, microscope images (recorded in reflective mode) at the corresponding temperatures are shown. For the AMP based ink, it can be noted easily that a lot of residuals originating from the AMP ligand are still present inside the deposition at lower temperatures (≤ 100 °C), whereas the spectra at 120 °C explicitly show no large contributions from vibrationally active species. A detailed analysis of the spectra and the associated signals is presented in Table S1. At 60 °C, the peaks corresponding to the carboxylate groups (for both formate and acetate) and the AMP O-H and N-H stretch vibrations above 3000 cm^{-1} are similar in intensity whereas this intensity ratio (carboxylate/AMP N-H and O-H stretch) decreases upon heating to 70-80 °C. This evolution suggests that carboxylate decomposition is initiated at low temperatures. Moreover, the strong difference between the 100 °C and 120 °C spectrum clarifies the distinct decreasing trend in sheet resistance (Figure 4) as AMP and carboxylate residuals are removed. Moreover, the organic residuals can be partly reduced to graphite-like structures as a peak at 1628 cm^{-1} is present. In the microscope images, the contribution of dark regions inside the deposited layers considerably shrinks in the entire observed temperature range. Therefore, it can be

postulated that these dark regions are in fact carbon-rich residuals originating from the amine ligands. For the hexylamine based ink, the principal evolution in the infrared spectra takes place at lower temperatures (60 – 70 °C, See figure S9), which also explains the less evident decrease in sheet resistance in the investigated temperature interval (80 – 120 °C). The fact that the layers acquired from $Ag(hex)_x$ inks are more performant in the low range of the defined temperature window (around 80 °C), can even be checked visually by considering their respective optical microscope images: the occurrence of dark (less reflective) regions in the image is remarkably lower (but decreases further upon heating, Figure S9)

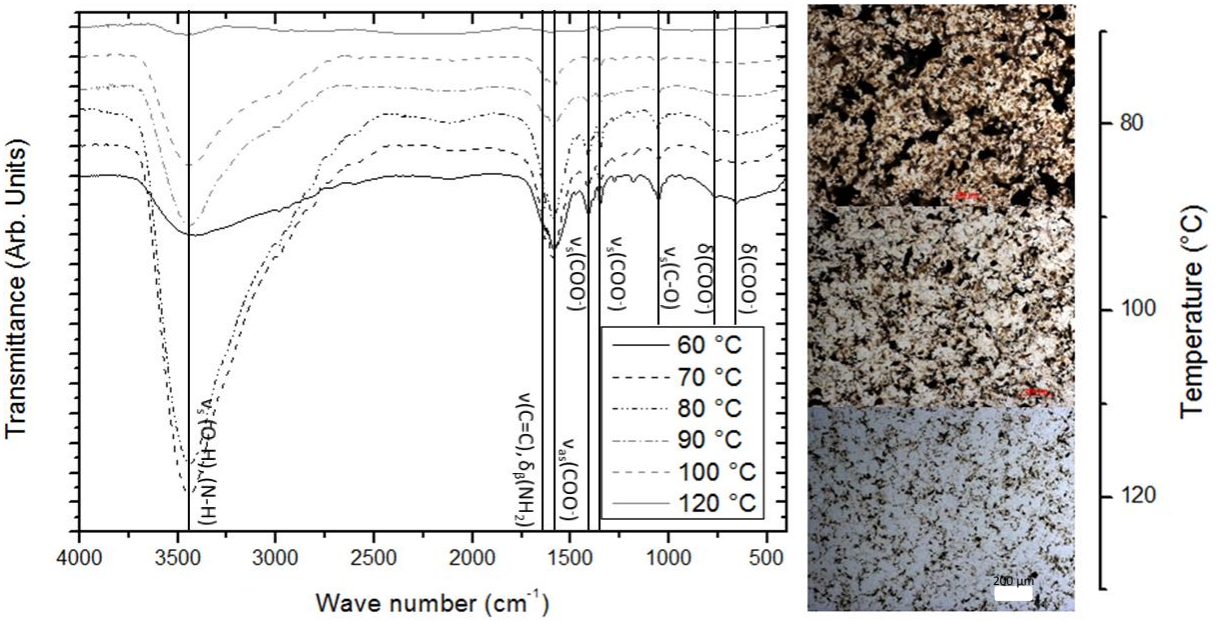

Figure 5: Evolution of FTIR spectra for the $Ag(AMP)_x$ ink at different deposition temperatures (left). The removal of organics towards higher temperatures can be observed and is further illustrated by the optical microscope images (right).A detailed analysis and assignment of the infrared signals (based on [63,64]), can be found in the supporting information (Table S1)

To verify whether the dark areas in the microscope images correspond to undecomposed organic content of the layers, a SEM/EDX study was performed. For this purpose, a silver layer with a clear segregation between the two different area types was selected for analysis, like the Ag(AMP) ink layer treated at 80 °C shown above. The distinction between both zones with an assumed difference in composition is also manifest in electron microscopy images (Figure 6). The EDX probed areas are indicated on the SEM image with squares (a) and (b) and their respective EDX spectra confirm our hypothesis: the dark area (b) is characterized by an elevated carbon content whereas the EDX of the (a) region shows the dominant presence of silver. The exact position of the EDX measurement can be verified via Figure S10 in the supporting information as the electron beam leaves marks on the surface. Moreover, a detailed image of the silver deposition morphology is included (Figure S11), showing a complete coverage of the surface with small grains. Eventually, the reduced presence of the (b) zones at increased temperatures (100 – 120 °C) is consistent with the observations in FTIR and sheet resistance values mentioned earlier. A similar analysis was performed on a silver layer deposited at 120 °C from a $Ag(hex)_x$ ink. Although the incidence of dark carbon-rich regions is significantly lower, the segregation between silver and carbon dominated regions could be confirmed (Figure S12).

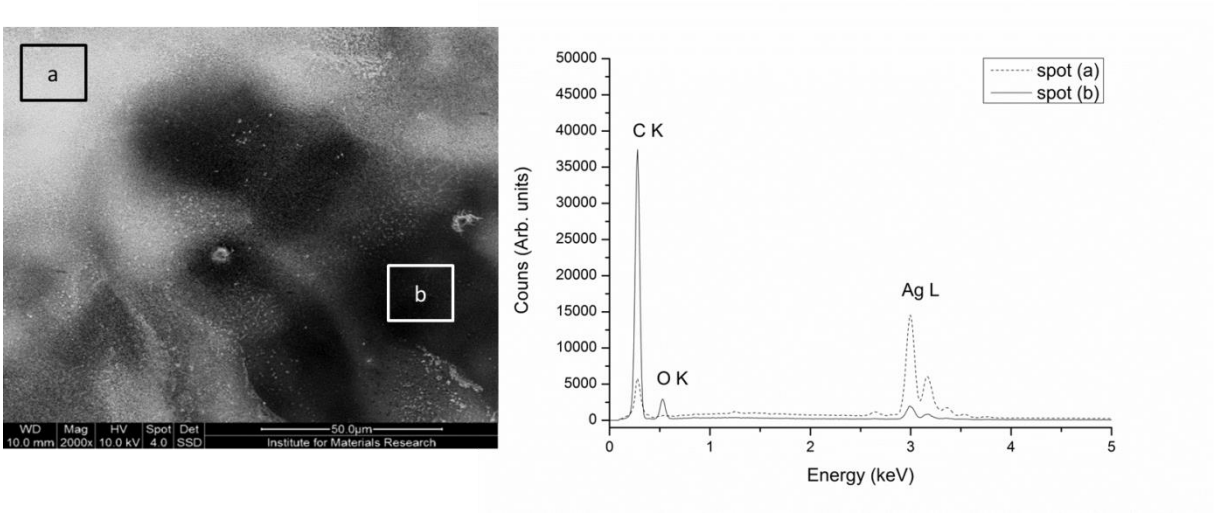

Figure 6: SEM image of a silver layer deposited at 80 °C from a Ag(AMP)$_x$ based ink (left). The EDX spectra corresponding to the highlighted areas (a) and (b) illustrate the difference in local composition (right). Part of the C K and O K peaks can be due to the underlying PET substrate. The EDX spectrum was collected with an acceleration voltage of 5 kV to decrease the contribution of the underlying PET as layers were estimated to have a thickness around 0.1 micron (see further).

Besides EDX, the elemental inhomogeneity could also be illustrated via peak force quantitative nanoscale mechanical characterization (PF-QNM™). As the AFM tip makes direct contact with the probed surface, the adhesion between the tip and the local features of the silver layer can be measured, based on the interpretation of force-distance curves. Different materials exhibit diverse adhesion values, allowing us to distinguish between the carbon-rich and carbon-deficient regions. Figure S13 illustrates that the carbon-rich (B) regions are identified unambiguously as higher adhesion values can be extracted, compared to regions which clearly show a morphology related to silver grains (A). Combining both EDX and PF-QNM measurements also shows that the carbon rich zones extend from the bulk (determined via EDX with an acceleration voltage of 5 kV, so penetration of the entire silver layer is plausible) to the surface. Moreover, the organic residue regions can be recognized in the profiles, as they exhibit gradual height-increasing features, resulting in an overall increase of surface roughness values. The transitions between the organic residuals and the silver grain dominated regions are suffering from huge height fluctuations (as illustrated extensively in supporting information Figure S14 for both Ag(hex)$_x$ and Ag(AMP)$_x$ ink layers). Therefore, the heat-induced removal of organic leftovers is considered to be beneficial for both the conductivity as well as the roughness of the resulting silver layers. The effect of the increasing temperature on the roughness of the Ag(hex)$_x$ and Ag(AMP)$_x$ ink layers is shown in Figure 7. The evolution in surface roughness and the variation in roughness on different measurements spots is more pronounced for the Ag(AMP)$_x$ inks because of its higher residual organic content at 80 °C (so more organic removal in the 80 – 120 °C interval). We can conclude that the optimal deposition temperature for both inks is 120 °C (on the condition that substrate cannot withstand higher temperatures).

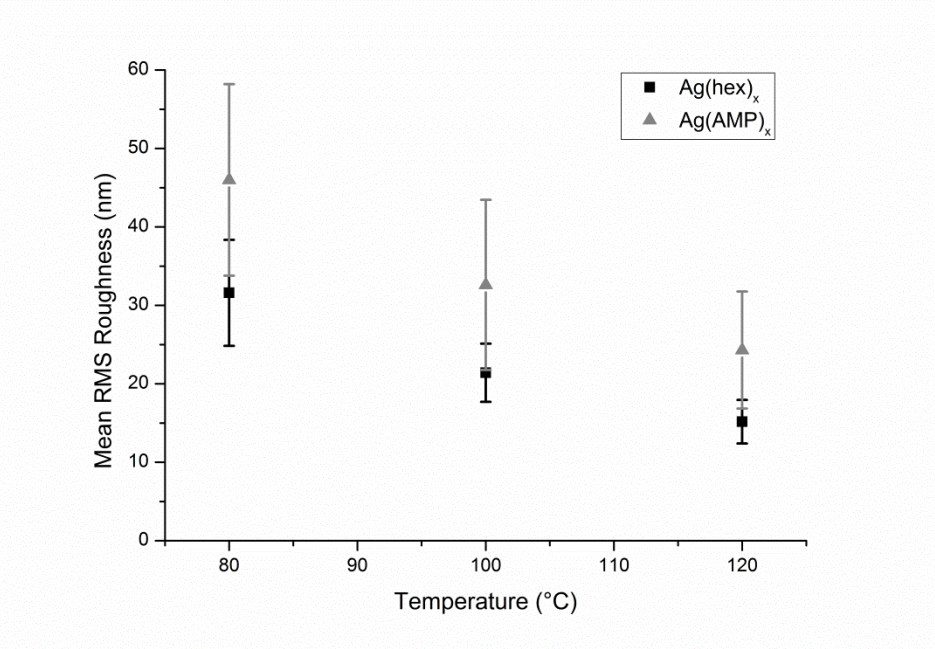

Figure 7: The surface roughness as a function of deposition temperature shows that the removal of organic residues has a beneficial effect on the morphology. Silver layers obtained from 100 % ethanol based inks on PET are shown. RMS average values for at least 4 measurements of different sample spots are plotted.

Even at 120 °C, a RMS roughness of 15-20 nm remains. Both SEM and AFM images indicate the local occurrence of a more granulated silver structure (Figure 8). Silver layers resulting from all tested MOD inks reveal these imperfections in the entire investigated temperature range. The formation of these agglomerates is ascribed to the mono-solvent composition of the inks, with a relatively low boiling point (ethanol). Evaporation takes place very quickly during the deposition process, which can lead to an uneven silver deposition. Addition of solvents with higher boiling points can possibly remediate this effect. However, a solvent optimization study is beyond the scope of this article.

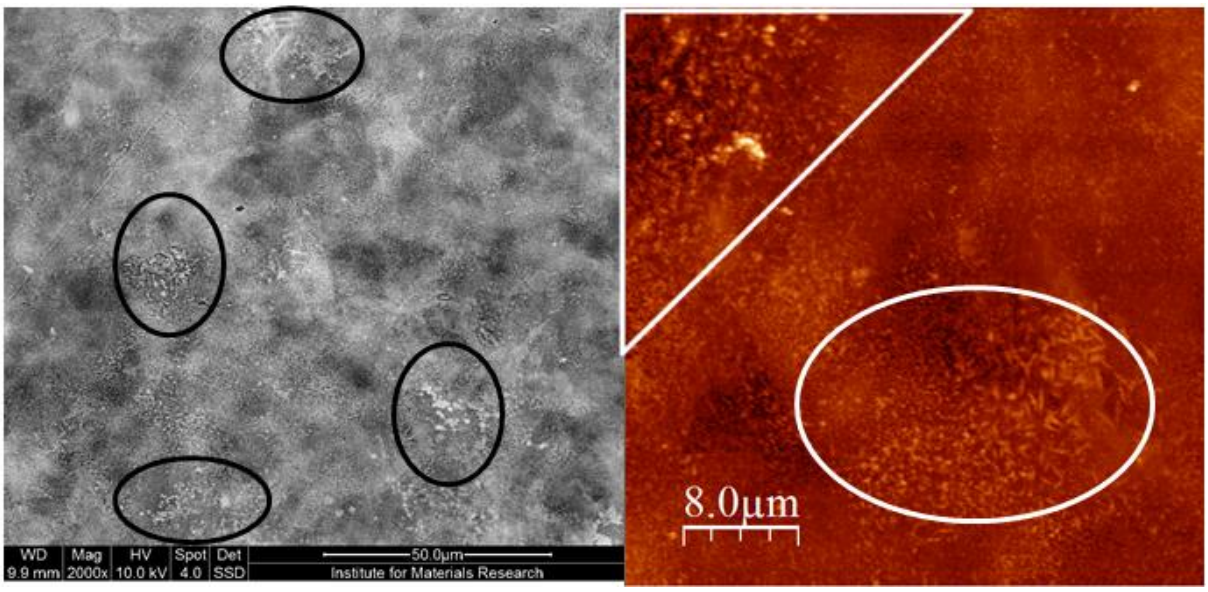

Figure 8: SEM (left) and AFM (right) image of a silver layer deposited at 120 °C from an $Ag(hex)_x$ based ink. The areas showing an increased roughness due to irregular silver deposition are marked.

The use of the USSC technique allowed for depositing silver layers with various thicknesses as a function of the amount of passes and the dispensing flow. If the amount of nozzle passes or the dispense flow was decreased, semi-transparent layers could be obtained. Figure 9 illustrates the transmittance of visible light for different spray coat parameters. It can be clearly observed that the thickness and thus the transparency of the layer affects the sheet resistance: for very thin silver layers (5 passes), the silver deposition is discontinuous consisting of silver islands and no conductivity could be measured. The semi-transparent properties are illustrated further (Figure 9 inset) for the silver layers deposited via 15 passes with a dispensing flow of 0.25 ml/min. The tunability of the layer thickness allows for future studies to optimize the conductivity-transparency trade-off, also involving solvent blend optimization.

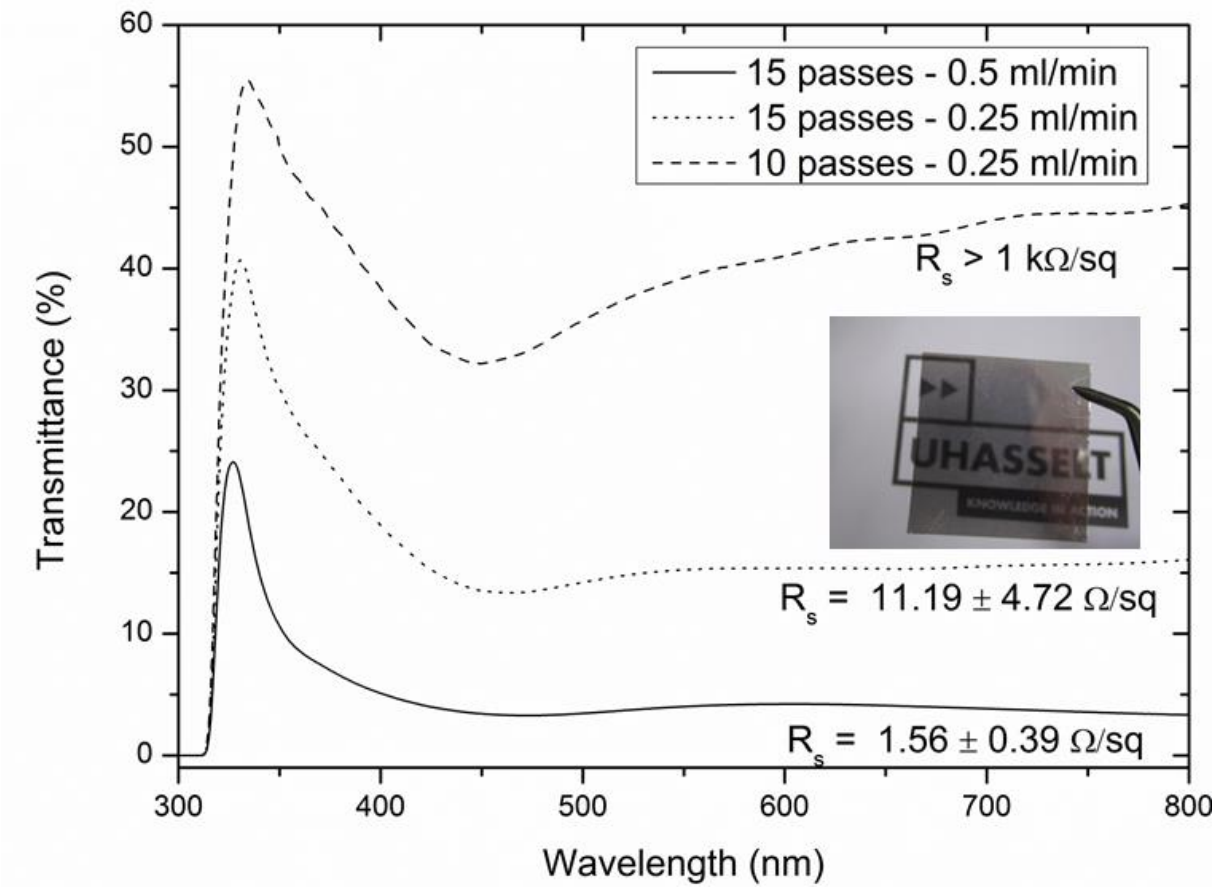

Figure 9: UV-VIS transmittance for silver layers deposited from the $Ag(hex)_x$ ink at 120 °C in pure ethanol. The sheet resistance decreases upon transmittance increase. Note that the USSC parameters differ from the default values mentioned in the experimental part. This was done to vary the thickness of the silver layers. The image (inset) demonstrates the transparency of the 15 passes layer with a 0.25 ml/min flowrate (11.19 Ω/ sq sheet resistance).

X-TEM measurements were performed analyzing the silver deposition from $Ag(hex)_x$ inks on PET to extract the thickness of the layers. Figure 10 shows that the thickness of the silver layer, deposited at 120 °C according to the spray coat parameters described in the experimental section, can be estimated to be 110 ± 20 nm. Combining the sheet resistance of 0.99 ± 0.17 Ω/sq, and thickness, the resistivity of the layers was calculated to be approximately $(10.9 \pm 2.7)\cdot10^{-8}$ Ω·m, which is 6.85 times the bulk resistivity of silver ($1.59\cdot10^{-8}$ Ω·m). These values are competitive to state of the art literature on silver MOD inks [32,41], reporting $7.44 \cdot10^{-8}$ Ω·m and $7.3\cdot10^{-8}$ Ω·m respectively. X-TEM images of silver layers deposited at 70 °C from a $Ag(hex)_x$ MOD ink illustrate once more the roughness increase

due to the incomplete ink decomposition, which makes it tedious to extract a reliable value for the layer thickness and thus the resistivity (Figure S15). The limited silver-silver adhesion for $Ag(NH_3)_2^+$ inks could also be exemplified as the silver depositions peel off during X-TEM sample preparation via microtome cutting (Figure S15).

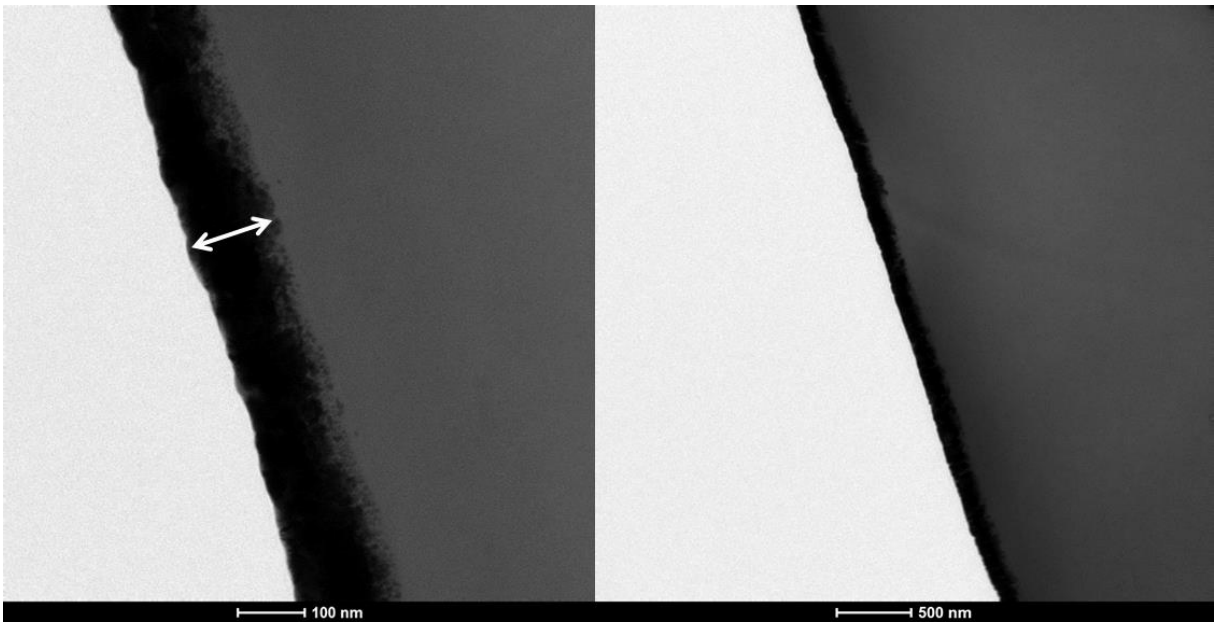

Figure 10: X-TEM images of $Ag(hex)_x$ inks depositions (120 °C) on PET substrates prepared via cryomicrotome cutting.

Conclusion

Silver MOD inks for USSC applications were successfully designed, inspired by various inkjet MOD inks reported in literature. In order to prolong the ink stability, the use of primary amine ligands and storage in cooled environments is recommended. Highly-conductive silver layers could be obtained from all low-temperature reducing silver complexes in a temperature window from 70 °C to 120 °C. The layer morphology (roughness) and sheet resistance were used as evaluation criteria to select the most promising MOD inks: $Ag(hex)_x$ complex based inks yielded layers with a resistivity of $10.9 \cdot 10^{-8}$ $\Omega \cdot m$ (15 % of bulk silver conductivity). In summary, the fact that such smooth (15.2 nm RMS), thin (110 nm) and highly-conductive layers can be obtained in a time-efficient way with the unique USSC - MOD ink combination may be considered as a huge step forward in the printable electronics research. Moreover, the ultrasonic spray coating of the $Ag(hex)_x$ ink allows us to deposit semi-transparent layers with a tunable thickness and excellent adhesion on PET substrates, without post annealing steps. Further improvements may be expected from an optimization of the solvent blend and spray coat parameters, aspiring transparent, highly conductive features. Moreover, the new developed inks hold promise for industrial application in fast R2R processing and open possibilities to coat 3D and/or flexible heat-sensitive surfaces.

Acknowledgements

The work was supported by the FWO, the Research Foundation of Flanders [project G041913N] and the BOF doctoral fund of Hasselt University. The author would also like to thank Ilaria Cardinaletti for the AFM support and Giulia Maino for the advice on the electrochemical experiments.

References

1. Stempien, Z.; Rybicki, E.; Rybicki, T.; Lesnikowski, J. Inkjet-printing deposition of silver electro-conductive layers on textile substrates at low sintering temperature by using an aqueous silver ions-containing ink for textronic applications. *Sensors and Actuators B: Chemical* **2016**, *224*, 714-725.
2. Wang, J.; Jiu, J.; Nogi, M.; Sugahara, T.; Nagao, S.; Koga, H.; He, P.; Suganuma, K. A highly sensitive and flexible pressure sensor with electrodes and elastomeric interlayer containing silver nanowires. *Nanoscale* **2015**, *7*, 2926-2932.
3. Chen, T.G.; Huang, B.Y.; Liu, H.W.; Huang, Y.Y.; Pan, H.T.; Meng, H.F.; Yu, P. Flexible silver nanowire meshes for high-efficiency microtextured organic-silicon hybrid photovoltaics. *ACS Applied Materials & Interfaces* **2012**, *4*, 6857-6864.
4. Sanchez-Romaguera, V.; Ziai, M.A.; Oyeka, D.; Barbosa, S.; Wheeler, J.S.R.; Batchelor, J.C.; Parker, E.A.; Yeates, S.G. Towards inkjet-printed low cost passive UHF RFID skin mounted tattoo paper tags based on silver nanoparticle inks. *Journal of Materials Chemistry C* **2013**, *1*, 6395.
5. Krebs, F.C. Fabrication and processing of polymer solar cells: A review of printing and coating techniques. *Solar Energy Materials and Solar Cells* **2009**, *93*, 394-412.
6. Singh, M.; Haverinen, H.M.; Dhagat, P.; Jabbour, G.E. Inkjet printing-process and its applications. *Advanced materials* **2010**, *22*, 673-685.
7. Cummins, G.; Desmulliez, M.P.Y. Inkjet printing of conductive materials: A review. *Circuit World* **2012**, *38*, 193-213.
8. van Osch, T.H.J.; Perelaer, J.; de Laat, A.W.M.; Schubert, U.S. Inkjet printing of narrow conductive tracks on untreated polymeric substrates. *Advanced materials* **2008**, *20*, 343-345.
9. Tehrani, Z.; Korochkina, T.; Govindarajan, S.; Thomas, D.J.; O'Mahony, J.; Kettle, J.; Claypole, T.C.; Gethin, D.T. Ultra-thin flexible screen printed rechargeable polymer battery for wearable electronic applications. *Organic Electronics* **2015**, *26*, 386-394.
10. Dang, M.C.; Dang, T.M.D.; Fribourg-Blanc, E. Silver nanoparticles ink synthesis for conductive patterns fabrication using inkjet printing technology. *Advances in Natural Sciences: Nanoscience and Nanotechnology* **2014**, *6*, 015003.
11. Fromm, J.E. Numerical calculation of the fluid dynamics of drop-on-demand jets. *IBM Journal of Research and Development* **1984**, *28*, 322-333.
12. Singh, A.; Katiyar, M.; Garg, A. Understanding the formation of PEDOT:PSS films by ink-jet printing for organic solar cell applications. *RSC Advances* **2015**, *5*, 78677-78685.
13. Shameli, K.; Ahmad, M.B.; Jazayeri, S.D.; Sedaghat, S.; Shabanzadeh, P.; Jahangirian, H.; Mahdavi, M.; Abdollahi, Y. Synthesis and characterization of polyethylene glycol mediated silver nanoparticles by the green method. *International journal of molecular sciences* **2012**, *13*, 6639-6650.
14. Vandevenne, G.; Marchal, W.; Verboven, I.; Drijkoningen, J.; D'Haen, J.; Van Bael, M.K.; Hardy, A.; Deferme, W. A study on the thermal sintering process of silver nanoparticle inkjet inks to achieve smooth and highly conducting silver layers. *Physica Status Solidi (a)* **2016**, *213*, 1403-1409.
15. Alshehri, A.H.; Jakubowska, M.; Mlozniak, A.; Horaczek, M.; Rudka, D.; Free, C.; Carey, J.D. Enhanced electrical conductivity of silver nanoparticles for high frequency electronic applications. *ACS applied materials & interfaces* **2012**, *4*, 7007-7010.
16. Vo, D.Q.; Shin, E.W.; Kim, J.S.; Kim, S. Low-temperature preparation of highly conductive thin films from acrylic acid-stabilized silver nanoparticles prepared through ligand exchange. *Langmuir* **2010**, *26*, 17435-17443.
17. Kim, D.; Moon, J. Highly conductive ink jet printed films of nanosilver particles for printable electronics. *Electrochemical and Solid-State Letters* **2005**, *8*, J30.

18. Fuller, S.B.; Wilhelm, E.J.; Jacobson, J.M. Ink-jet printed nanoparticle microelectromechanical systems. *Journal of Microelectromechanical systems* **2002**, *11*, 54-60.
19. Jackson, C.L.; McKenna, G.B. The melting behavior of organic materials confined in porous solids. *Journal of Chemical Physics* **1990**, *93*, 9002.
20. Magdassi, S.; Grouchko, M.; Berezin, O.; Kamyshny, A. Triggering the sintering of silver nanoparticles at room temperature. *ACS Nano* **2010**, *4*, 1943-1948.
21. Yeshchenko, O.A.; Dmitruk, I.M.; Alexeenko, A.A.; Kotko, A.V. Surface plasmon as a probe for melting of silver nanoparticles. *Nanotechnology* **2010**, *21*, 045203.
22. Tobjörk, D.; Aarnio, H.; Pulkkinen, P.; Bollström, R.; Määttänen, A.; Ihalainen, P.; Mäkelä, T.; Peltonen, J.; Toivakka, M.; Tenhu, H.*, et al.* IR-sintering of ink-jet printed metal-nanoparticles on paper. *Thin Solid Films* **2012**, *520*, 2949-2955.
23. Ko, S.H.; Pan, H.; Grigoropoulos, C.P.; Luscombe, C.K.; Fréchet, J.M.J.; Poulikakos, D. All-inkjet-printed flexible electronics fabrication on a polymer substrate by low-temperature high-resolution selective laser sintering of metal nanoparticles. *Nanotechnology* **2007**, *18*, 345202.
24. Cherrington, M.; Claypole, T.C.; Gethin, D.T.; Worsley, D.A.; Deganello, D. Non-contact assessment of electrical performance for rapidly sintered nanoparticle silver coatings through colorimetry. *Thin Solid Films* **2012**, *522*, 412-414.
25. Jahn, S.F.; Blaudeck, T.; Baumann, R.R.; Jakob, A.; Ecorchard, P.; Rüffer, T.; Lang, H.; Schmidt, P. Inkjet printing of conductive silver patterns by using the first aqueous particle-free mod ink without additional stabilizing ligands. *Chemistry of Materials* **2010**, *22*, 3067-3071.
26. Park, S.-H.; Jang, S.; Lee, D.-J.; Oh, J.; Kim, H.-S. Two-step flash light sintering process for crack-free inkjet-printed ag films. *Journal of Micromechanics and Microengineering* **2013**, *23*, 015013.
27. Chung, W.H.; Hwang, H.J.; Lee, S.H.; Kim, H.S. In situ monitoring of a flash light sintering process using silver nano-ink for producing flexible electronics. *Nanotechnology* **2013**, *24*, 035202.
28. Grouchko, M.; Kamyshny, A.; Mihailescu, C.F.; Anghel, D.F.; Magdassi, S. Conductive inks with a “built-in”mechanism that enables sintering at room temperature. *ACS Nano* **2011**, *5*, 3354-3359.
29. Wakuda, D.; Kim, K.; Suganuma, K. Room temperature sintering of ag nanoparticles by drying solvent. *Scripta Materialia* **2008**, *59*, 649-652.
30. Jahn, S.F.; Jakob, A.; Blaudeck, T.; Schmidt, P.; Lang, H.; Baumann, R.R. Inkjet printing of conductive patterns with an aqueous solution of $[AgO_2C(CH_2OCH_2)_3H]$ without any additional stabilizing ligands. *Thin Solid Films* **2010**, *518*, 3218-3222.
31. Curtis, C.J., Rivkin, T, Miedaner, A., Alleman, J.Perkins, J., Smith, L., Ginley, D.S. Direct-write printing of silver metallizations on silicon solar cells. *MRS proceedings* **2002**, 79-84.
32. Chen, C.-N.; Dong, T.-Y.; Chang, T.-C.; Chen, M.-C.; Tsai, H.-L.; Hwang, W.-S. Solution-based β-diketonate silver ink for direct printing of highly conductive features on a flexible substrate. *Journal of Materials Chemistry C* **2013**, *1*, 5161.
33. Krzewska, S.; Podsiadly, H. Complexes of Ag(I) with ligands containing sulfur donor atoms. *Polyhedron* **1986**, *5*, 937-944.
34. Walker, S.B.; Lewis, J.A. Reactive silver inks for patterning high-conductivity features at mild temperatures. *Journal of the American Chemical Society* **2012**, *134*, 1419-1421.
35. Wu, J.-T.; Hsu, S.L.-C.; Tsai, M.-H.; Hwang, W.-S. Inkjet printing of low-temperature cured silver patterns by using agno3/1-dimethylamino-2-propanol inks on polymer substrates. *The Journal of Physical Chemistry C* **2011**, *115*, 10940-10945.
36. Nie, X.; Wang, H.; Zou, J. Inkjet printing of silver citrate conductive ink on pet substrate. *Applied Surface Science* **2012**, *261*, 554-560.
37. Dong, Y.; Li, X.; Liu, S.; Zhu, Q.; Li, J.-G.; Sun, X. Facile synthesis of high silver content mod ink by using silver oxalate precursor for inkjet printing applications. *Thin Solid Films* **2015**, *589*, 381-387.

38. Black, K.; Singh, J.; Mehta, D.; Sung, S.; Sutcliffe, C.J.; Chalker, P.R. Silver ink formulations for sinter-free printing of conductive films. *Scientific reports* **2016**, *6*, 20814.
39. Chen, S.P.; Kao, Z.K.; Lin, J.L.; Liao, Y.C. Silver conductive features on flexible substrates from a thermally accelerated chain reaction at low sintering temperatures. *ACS applied materials & interfaces* **2012**, *4*, 7064-7068.
40. Fritsch, J.; Wisser, F.M.; Eckhardt, K.; Bon, V.; Mondin, G.; Schumm, B.; Grothe, J.; Kaskel, S. A new molecular silver precursor for the preparation of thin conductive silver films. *Journal of Physics and Chemistry of Solids* **2013**, *74*, 1546-1552.
41. Ahn, H.-Y.; Cha, J.-R.; Gong, M.-S. Preparation of sintered silver nanosheets by coating technique using silver carbamate complex. *Materials Chemistry and Physics* **2015**, *153*, 390-395.
42. Huang, Q.; Shen, W.; Song, W. Synthesis of colourless silver precursor ink for printing conductive patterns on silicon nitride substrates. *Applied Surface Science* **2012**, *258*, 7384-7388.
43. Wang, T.; Scarratt, N.W.; Yi, H.; Dunbar, A.D.F.; Pearson, A.J.; Watters, D.C.; Glen, T.S.; Brook, A.C.; Kingsley, J.; Buckley, A.R*., et al.* Fabricating high performance, donor-acceptor copolymer solar cells by spray-coating in air. *Advanced Energy Materials* **2013**, *3*, 505-512.
44. Girotto, C.; Moia, D.; Rand, B.P.; Heremans, P. High-performance organic solar cells with spray-coated hole-transport and active layers. *Advanced Functional Materials* **2011**, *21*, 64-72.
45. Tait, J.G.; Worfolk, B.J.; Maloney, S.A.; Hauger, T.C.; Elias, A.L.; Buriak, J.M.; Harris, K.D. Spray coated high-conductivity PEDOT:PSS transparent electrodes for stretchable and mechanically-robust organic solar cells. *Solar Energy Materials and Solar Cells* **2013**, *110*, 98-106.
46. Gilissen, K.; Stryckers, J.; Verstappen, P.; Drijkoningen, J.; Heintges, G.H.L.; Lutsen, L.; Manca, J.; Maes, W.; Deferme, W. Ultrasonic spray coating as deposition technique for the light-emitting layer in polymer leds. *Organic Electronics* **2015**, *20*, 31-35.
47. Zheng, Y.; Li, S.; Shi, W.; Yu, J. Spray-coated nanoscale conductive patterns based on in situ sintered silver nanoparticle inks. *Nanoscale Research Letters* **2014**, *9*, 1-7.
48. Reale, A.; La Notte, L.; Salamandra, L.; Polino, G.; Susanna, G.; Brown, T.M.; Brunetti, F.; Di Carlo, A. Spray coating for polymer solar cells: An up-to-date overview. *Energy Technology* **2015**, *3*, 385-406.
49. van den Ham, E.J.; Gielis, S.; Van Bael, M.K.; Hardy, A. Ultrasonic spray deposition of metal oxide films on high aspect ratio microstructures for three-dimensional all-solid-state Li-ion batteries. *ACS Energy Letters* **2016**, 1184-1188.
50. Tait, J.G.; Wong, C.; Cheyns, D.; Turbiez, M.; Rand, B.P.; Heremans, P. Ultrasonic spray coating of 6.5 % efficient diketopyrrolopyrrole-based organic photovoltaics. *IEEE Journal of Photovoltaics* **2014**, *4*, 1538-1544.
51. Girotto, C.; Rand, B.P.; Steudel, S.; Genoe, J.; Heremans, P. Nanoparticle-based, spray-coated silver top contacts for efficient polymer solar cells. *Organic Electronics* **2009**, *10*, 735-740.
52. Ankireddy, K.; Vunnam, S.; Kellar, J.; Cross, W. Highly conductive short chain carboxylic acid encapsulated silver nanoparticle based inks for direct write technology applications. *Journal of Materials Chemistry C* **2013**, *1*, 572-579.
53. Canepari, S.; Carunchio, V.; Castellano, P.; Messina, A. Protonation and silver(I) complex-formation equilibria of some amino-alcohols. *Talanta* **1997**, *44*, 2059-2067.
54. Del Piero, S.; Fedele, R.; Melchior, A.; Portanova, R.; Tolazzi, M.; Zangrando, E. Solvation effects on the stability of silver(I) complexes with pyridine-containing ligands studied by thermodynamic and DFT methods. *Inorganic chemistry* **2007**, *46*, 4683-4691.
55. Ansell, G.B. Crystal structure of a I: I complex between silver iodide and morphohe. *Perkin Trans.* **1976**, *1*, 104-106.
56. Paints and varnishes: Iso 2409. *International Standards* **1992**.

57. Zaarour, M.; El Roz, M.; Dong, B.; Retoux, R.; Aad, R.; Cardin, J.; Dufour, C.; Gourbilleau, F.; Gilson, J.P.; Mintova, S. Photochemical preparation of silver nanoparticles supported on zeolite crystals. *Langmuir* **2014**, *30*, 6250-6256.
58. Lu, H.W.; Liu, S.H.; Wang, X.L.; Qian, X.F.; Yin, J.; Zhu, Z.K. Silver nanocrystals by hyperbranched polyurethane-assisted photochemical reduction of Ag^{+}. *Materials Chemistry and Physics* **2003**, *81*, 104-107.
59. Giocondi, J.L.; Rohrer, G.S. Spatially selective photochemical reduction of silver on the surface of ferroelectric barium titanate. *Chemistry of Materials* **2001**, *13*, 241-242.
60. Slager, T.L.; Lindgren, B.J.; Mallman, A.J.; Greenler, R.G. The infrared spectra of the oxides and carbonates of silver. *Journal of Physical Chemistry* **1972**, *76*, 940-943.
61. Judd, M.D.; Plunkett, B.A.; Pope, M.I. The thermal decomposition of calcium, sodium, silver and copper(ii) acetates. *Journal of Thermal Analysis* **1974**, *6*, 555-563.
62. Logvinenko, V.; Polunina, O.; Mikhailov, Y.; Mikhailov, K.; Bokhonov, B. Study of thermal decomposition of silver acetate. *Journal of Thermal Analysis and Calorimetry* **2007**, *90*, 813-816.
63. Liao, L.F.; Lien, C.F.; Shieh, D.L.; Chen, M.T.; Lin, J.T. FTIR study of adsorption and photoassisted oxygen isotopic exchange of carbon monoxide, carbon dioxide, carbonate, and formate on TiO_2. *Journal of Physical Chemistry B* **2002**, *106*, 11240-11245.
64. Ito, K.; Bernstein, H.J. The vibrational spectra of the formate, acetate and oxalate ions. *Canadian Journal of Chemistry* **1955**, 170-177.